Compressive Performance of Steel Fibre Reinforced Concrete-Filled Plastic Tubes

Jen Hua Ling[1], Eric Kiing Hung Wong[2]
[1]Centre for Research of Innovation & Sustainable Development, School of Engineering and Technology, University of Technology Sarawak, 96000 Sibu, Sarawak, Malaysia. (lingjenhua@uts.edu.my)
[2]School of Engineering and Technology, University of Technology Sarawak, 96000 Sibu, Sarawak (bce22090002@student.uts.edu.my)

Abstract
This study investigates the compressive strength behaviour of concrete specimens with varying diameters (75 mm, 100 mm, and 150 mm), steel fibre contents (0%, 0.75%, and 1.5%), and confinement conditions using PVC tubes. A total of 54 cylindrical specimens were prepared across four groups: plain concrete (C), fibre-reinforced concrete (FC), plain concrete with PVC confinement (TC), and fibre-reinforced concrete with PVC confinement (TFC). Results showed that compressive strength increased with specimen diameter due to a fourfold increase in cross-sectional area and reduced slenderness (h/d ratio), with strength gains ranging from 4.3 to 5.4 times for unconfined specimens and 3.5 to 4.1 times for confined ones. However, in PVC-confined specimens, a decreasing 2t/d ratio with increasing diameter limited the confinement effectiveness. Steel fibres showed inconsistent effects on strength, likely due to poor workability and uneven distribution. PVC confinement generally enhanced compressive strength, particularly at 1.5% fibre content, with increases of 64%, 58%, and 45% for specimens with diameters of 75 mm, 100 mm, and 150 mm, respectively. Observed failure modes included bulging, shear, and tube bursting. Bulging was associated with more effective confinement. These findings highlight the importance of jointly considering geometric scaling and material parameters in the design of confined fibre-reinforced concrete elements.

Keyword: *confinement effect, compressive strength, steel fibre reinforced concrete, PVC tube*

I. INTRODUCTION
Interest in concrete-filled tubes (CFTs) has grown significantly, as reflected by the sharp rise in related publications (Ling and Omoregie, 2025). CFTs are composite structural elements formed by filling tubes with concrete (Azeez et al., 2018). They are widely used in high-rise buildings, bridges, and subways due to their high axial strength, stiffness, ductility, and good seismic performance (He et al., 2018). Additionally, CFTs offer advantages in constructability and project economy (Fakharifar and Chen, 2017). The tube acts as permanent formwork, supporting construction loads during concrete placement and eliminating the need for formwork removal, thus saving time and cost (Wang et al., 2022).

Among the various types, concrete-filled steel tubes (CFSTs) and concrete-filled FRP tubes (CFFTs) are the most studied (Fakharifar and Chen, 2017). Each has its limitations: steel is prone to corrosion (Wang and Yang, 2012), while FRPs have poor compressive performance (Nunna et al., 2023), exhibit brittle failure (Fakharifar and Chen, 2017), and involve high material and labour costs (Abdulla, 2017). Concrete-filled plastic tubes (CFPTs) have since emerged as low-cost, corrosion-resistant alternatives. However, plastic tubes like PVC, uPVC, and HDPE have low stiffness and strength, offering limited confinement and reduced axial load capacity.

To address this limitation, steel fibres (SF) can be added to the concrete, using steel fibre reinforced concrete (SFRC) as the infill material for CFPT. The fibres bridge cracks, distribute stress more evenly, and prevent crack propagation, significantly improving the tensile and flexural strength of concrete (Pham, 2025). Adding at least 1% steel fibres by volume to the concrete can also enhance the ductility and strength of CFST filled with ultra-high-strength concrete (UHSC) (Liew and Xiong, 2012). Lu et al. (2015) reported that steel fibres improve the composite action between the steel tube and concrete, with the strength enhancement more noticeable in thicker tubes but less effective as concrete strength increases. In contrast, Hoang et al. (2019) found greater benefits with thinner steel tubes and recommended using 1% steel fibres by volume in CFST columns with thinner tubes.

These conflicting findings suggest that the interaction between steel fibres and the confining

tube is complex and likely affected by multiple variables. Notably, existing studies focus primarily on CFST, where the steel tube provides high stiffness. It remains unclear whether similar benefits apply to CFPT, as plastic tubes have much lower stiffness. For example, the modulus of elasticity of PVC is about 1/50th that of steel (Fakharifar and Chen, 2016), which may lead to different tube-concrete interaction mechanisms. This gap in understanding highlights the need for further investigation.

Therefore, this study investigates the use of SFRC in CFPT to assess its structural performance and examine whether steel fibre reinforcement can compensate for the limited confinement provided by PVC tubes. Compressive strength tests were conducted on both confined and unconfined specimens, with varying specimen sizes and fibre contents, to evaluate load capacity and failure behaviour.

II. METHODS

A total of 54 specimens were prepared, each 305 ± 5 mm high (Table I and Figure 1). They had diameters of 75 mm, 100 mm, or 150 mm, and steel fibre content of 0%, 0.75%, or 1.5% by cement weight. Specimens C and FC were plain and steel fibre reinforced concrete without PVC confinement. Specimens TC and TFC were the same types of concrete confined in PVC tubes.

Concrete grade 25 was prepared in six batches. Batches 1 and 2, 3 and 4, and 5 and 6 were cast together to accommodate varying steel fibre content. The water-cement ratio was maintained at 0.58. A superplasticizer (Real Power Flow RPF 630) was added at 0.5% of the cement weight to improve workability. Mix proportions are provided in Table II. Ordinary Portland Cement (OPC) grade 42.5 was used as the binder. Granite (6.3–20 mm) was used as coarse aggregate, and river sand passing a 600 µm sieve as fine aggregate. Both aggregates were oven-dried at 105°C for 24 hours to ensure a consistent water-cement ratio. Each batch produced nine samples (three specimens, with three identical samples per specimen) and three cubes for testing.

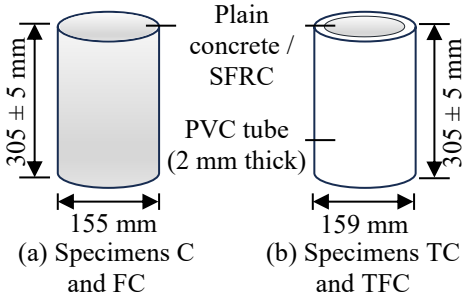

Figure 1. *Specimen designs*

TABLE I
Specification of Specimen with/without PVC Tube Incorporating Steel Fibres

Category	Specimen	PVC tube	Diameter, *d* (mm)	Steel Fibre content (%)
Plain concrete	C1	X	75	0
	C2	X	100	0
	C3	X	150	0
Steel fibre-reinforced concrete	FC1	X	75	0.75
	FC2	X	100	0.75
	FC3	X	150	0.75
	FC4	X	75	1.5
	FC5	X	100	1.5
	FC6	X	150	1.5
Plain concrete-filled plastic tube	TC1	√	75	0
	TC2	√	100	0
	TC3	√	150	0
Steel fibre reinforced concrete-filled plastic tube	TFC1	√	75	0.75
	TFC2	√	100	0.75
	TFC3	√	150	0.75
	TFC4	√	75	1.5
	TFC5	√	100	1.5
	TFC6	√	150	1.5

Note: C – Concrete, F – steel fibre reinforced, T – PVC tubed. Three samples were prepared and tested for each specimen, resulting in a total of 54 samples.

TABLE II
Mix Design for Specimen and Cube

Batch	Specimens	Steel fibre (g)	Water (kg)	Cement (kg)	Sand (kg)	Aggregate (kg)	Superplasticizer (ml)
1	C1 to C3	0	7.74	13.38	28.06	49.92	70
2	TC1 to TC3	0	7.74	13.38	28.06	49.92	70
3	FC1 to FC3	100.33	7.74	13.38	28.06	49.92	70
4	TFC1 to FTC3	100.33	7.74	13.38	28.06	49.92	70
5	FC4 to FC6	200.66	7.74	13.38	28.06	49.92	70
6	TFC4 to FTC6	200.66	7.74	13.38	28.06	49.92	70

Hooked-end steel fibres (0.55 mm diameter, 35 mm length) were added to the mix at 0%, 0.75%, or 1.5% by cement weight (Figure 2). According to the manufacturer, their nominal tensile strength was 1200 N/mm^2. The fibres were thoroughly mixed into the concrete to ensure uniform distribution before placement in the PVC tubes.

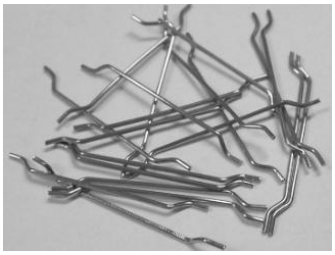

Figure 2. *Hooked-end steel fibre*

PVC tubes (155 mm inner diameter, 2 mm thick) were cut and used as moulds for all specimens (Figure 3). The bottoms were sealed with plastic and cellophane tape to prevent leakage. Concrete was poured in three equal layers, with each layer compacted using a tamping rod.

After casting, all specimens were left to set for 24 hours. For unconfined specimens (C and FC), the PVC moulds were removed. To minimise damage during removal, the moulds were pre-cut longitudinally and sealed externally with tape. For confined specimens (TC and TFC), the PVC tubes were retained as part of the CFPT. All specimens were then cured in water at room temperature for 28 days before testing.

The testing program began with material tests to verify the consistency and quality of materials (Table III and Figure 4). These results served as reference values for all specimens (C, FC, TC, and TFC). Slump and cube tests (150 mm) were performed on each batch to assess workability and compressive strength. A tensile test was also conducted to determine the tensile strength of the PVC tubes.

(a) Oven-drying aggregate (b) Sieving aggregate (c) Cutting PVC tube (d) Casting of specimens (e) Curing specimens

Figure 3. *Process of preparing specimens*

(a) Concrete slump test (b) Concrete cube compression test (c) PVC tube tensile test (d) Specimen compression test

Figure 4. *Testing program*

(a) Drum mixer (b) Universal Testing Machine (INSPEKT 300-1) (c) ELE International Compression Machine (d) Universal Testing Machine (MTS 64.206)

Figure 5. *Equipment used*

TABLE III
Test Program

Sample	Test Conducted	Purpose	Standard Referred	Testing Equipment
Concrete	Slump test	To assess the workability of fresh concrete in each batch	ASTM C143	Standard slump test set
	Cube compression test (150 mm)	To determine the compressive strength of each concrete batch	BS EN 12390-3	ELE International Compression Machine, ADR Auto V2.0, 2000 kN capacity
PVC tube	Tensile test	To measure the tensile strength of the PVC tube	ASTM D638	Universal Testing Machine, Inspekt 300-1, 300 kN capacity
FRC and CFPT specimens	Compression test	To determine the compressive strength of specimens C, FC, TC, and TFC	-	Universal Testing Machine, MTS 64.206, 2000 kN capacity

Compressive tests were then carried out on specimens C, FC, TC, and TFC to evaluate the effects of steel fibres on fibre-reinforced concrete (FRC) and concrete-filled plastic tubes (CFPTs). A Universal Testing Machine (Figure 5(d)) applied compressive load at a constant rate of 0.10 mm/s until failure. Load and displacement were recorded, and failure modes were observed.

III. RESULTS AND DISCUSSIONS

A. Workability of SFRC

Table IV shows the slump test results for each concrete batch, ranging from 9 mm to 31.75 mm. This indicates that the mixes were relatively dry with low workability, despite the use of a superplasticizer and a high water-cement ratio of 0.58. Such low workability is unsuitable for CFPT columns, which require vertical casting in slender forms with limited space in actual practice, increasing the risk of poor compaction, honeycombing, and reduced structural performance.

TABLE IV
Slump test and Concrete Cube Test Results

Batch no.	Specimens	Steel Fibre (%)	Average slump (mm)
1 and 2	C1 to C3 and TC1 to TC3	0	31.75
3 and 4	FC1 to FC3 and TFC1 to FTC3	0.75	31.5
5 and 6	FC4 to FC6 and TFC4 to FTC6	1.5	9

The low workability was likely caused by the use of oven-dried coarse and fine aggregates. This approach was intended to maintain a consistent water-cement ratio across batches by eliminating variations from surface moisture. However, the dry aggregates may have absorbed water and superplasticizer during mixing, reducing the free water available to lubricate the mix. Aggregates with high water absorption can lower the effective water-cement ratio, leading to poor consistency and reduced workability (Nedeljković et al., 2021).

To address this issue, trial mixes should be carried out using surface-dried aggregates before actual batching to determine an appropriate water-cement ratio, rather than relying solely on calculated values from the mix design. This allows for necessary water adjustments to ensure adequate workability and consistency, especially when steel fibres are used. Poor workability can lead to inadequate compaction, segregation, or honeycombing, which may distort test results and misrepresent the actual structural performance. Conducting trial mixes with controlled aggregate moisture helps ensure consistent quality and enhances the reliability and validity of the experimental data.

Workability decreased as steel fibre content increased (Table IV). Batches 1 and 2 (0% steel fibre) had a slump of 31.75 mm, which dropped to 9 mm in batches 5 and 6 with 1.5% fibre. This trend agrees with earlier findings; Ulas et al. (2017) reported zero slump for SFRC with 1% fibre, while Khaloo et al. (2014) noted a general reduction in workability with increasing fibre content.

Steel fibres increase the surface area requiring wetting, reducing the free water available to lubricate cement particles (Wang et al., 2021). Their dry surfaces absorb part of the mixing water, lowering workability and flowability (El-Dieb and Reda Taha, 2012). Deformed fibres, such as hooked-end or crimped types, also increase friction and interlock with aggregates, further reducing workability (Pham, 2025). Wu et al. (2016) found that in UHPC with 3% steel fibres, flowability dropped by 45.1% with corrugated fibres and 51.2% with hooked-end fibres, compared to straight ones.

Akeed et al. (2022) classified fibres into elastic and rigid types. Rigid fibres, such as steel fibres, tend to increase yield stress, while flexible fibres like polypropylene and polyvinyl alcohol

fibres allow higher viscosity. In this study, rigid steel fibres were used. Their hooked ends enhanced yield stress compared to straight fibres due to both cohesive and anchoring effects. However, the deformed shape reduced the rheological performance of the concrete by increasing internal friction and interlocking.

Low workability is undesirable as it makes concrete harder to place and compact, increasing the risk of honeycombing and air voids. These defects reduce the effective load-bearing area and lead to stress concentrations. Khaloo et al. (2014) noted that reduced workability can lower compaction levels, which subsequently decreases concrete strength.

B. Compressive Strength of SFRC

Table V shows that all concrete batches met the design strength of 25 N/mm^2, with average compressive strengths ranging from 30.7 to 37.1 N/mm^2. This higher strength was achieved by designing the mix for a target mean strength of 38.12 N/mm^2, based on standard procedures to ensure that at least 95% of the concrete would exceed 25 N/mm^2.

TABLE V
Compressive strength of concrete cube at 28th days (N/mm^2)

Batch no.	Specimen	Cube Sample 1	Cube Sample 2	Cube Sample 3	Average
1	C1 to C3	39.0	37.0	35.3	37.1
2	TC1 to TC3	36.3	34.3	30.5	33.7
3	FC1 to FC3	27.9	33.0	31.2	30.7
4	TFC1 to FTC3	30.7	36.5	29.0	32.1
5	FC4 to FC6	33.6	34.5	35.0	34.4
6	TFC4 to FTC6	26.8	28.8	39.0	31.5

TABLE VI
Tensile Test Result of PVC Tube

Specimen	Area (mm^2)	Yield Load (N)	Yield Strength (N/mm^2)	Ultimate Load (N)	Ultimate Strength (N/mm^2)
Sample 1	27.02	689.7	25.5	755.7	28.0
Sample 2	26.11	697.9	26.7	762.3	29.2
Sample 3	29.11	774.3	26.6	848.4	29.1
Average	-	-	26.3	-	28.8

A low water-cement ratio may improve concrete strength. Zheng et al. (2021) reported that a higher water-cement ratio increases the volume of pores and capillaries, leading to lower compressive strength. However, this benefit depends on achieving adequate workability, which may not have been the case in this study. The concrete exhibited relatively low workability (Table IV), likely due to excessive water absorption by oven-dried aggregates during mixing, which may have compromised compaction quality.

Notable fluctuations were observed in the cube compressive strength, despite using three identical samples. Batch 6, which contained 1.5% steel fibre, showed the largest variation, with values ranging from 26.8 to 39 N/mm^2. This suggests possible inconsistencies in the mix, which may be due to uneven distribution of materials (cement, water, aggregates, fibres), poor workability, or inconsistent compaction during casting.

C. Tensile Strength of PVC tube

Table VI shows that the tensile strength of the three PVC samples was consistent, averaging 28.8 N/mm^2. This is approximately 1/10 of the tensile strength of mild steel tubes, which ranges from 250 to 300 N/mm^2. The elastic modulus of PVC is also much lower, at about 1/5 of concrete and 1/50 of steel (Abdulla, 2017). As a result, PVC tubes carry less axial load and provide weaker confinement compared to steel tubes (Fakharifar and Chen, 2016). Mohammad Askari et al., (2020) reported that the confining effect of UPVC is similar to that of PVC but significantly lower than that of steel. Therefore, the strength improvement by PVC tubes is expected to be rather limited.

This limitation can be partially addressed by using thicker tubes, but the improvement is limited by the low modulus of elasticity. Wang and Yang (2012) reported that increasing the thickness of PVC tubes enhances the axial strength and ductility of concrete-filled tubes.

Likewise, Bandyopadhyay et al. (2019) found that thicker UPVC tubes slightly improve the load-bearing capacity of both plain and fibre-reinforced concrete, although the effect remains limited due to the material's low stiffness. In this study, all TC and TFC specimens used a constant PVC tube thickness of 2 mm. Therefore, the effect of tube thickness was not examined.

D. Test Results of Specimens

Table VII presents the compressive strength results for specimens C, FC, TC, and TFC, each based on three identical samples. The average values were grouped by steel fibre content, specimen diameter, and the presence of a PVC tube to illustrate the parametric response in Table VIII. The effects of these parameters on compressive strength are clearly observed.

Effect of Specimen Diameter

Compressive strength increased with specimen diameter, regardless of steel fibre content or the presence of PVC tubes (Table VIII). For example, at 1.5% steel fibre, strength increased from 83.3 kN to 359.6 kN without PVC tubes, and from 136.7 kN to 521.2 kN with tubes. This trend is expected, as a larger diameter provides a greater load-bearing area. When the diameter, *d*, increased from 75 mm to 150 mm, the cross-sectional area became four times larger. This geometric increase aligns reasonably well with the observed strength gains, which ranged from 4.3 to 5.4 times without PVC tubes and from 3.5 to 4.1 times with tubes (Table IX).

TABLE VII
Compressive strength of specimen (kN)

Specimen	Sample 1	Sample 2	Sample 3	Average
C1	92.1	95.4	115.4	101.0
C2	143.7	261.0	238.8	214.5
C3	475.2	514.6	495.8	495.2
FC1	80.7	68.7	102.8	84.1
FC2	177.5	93.8	195.0	155.4
FC3	508.3	440.4	418.6	455.8
FC4	75.2	73.2	101.7	83.3
FC5	153.3	161.1	140.6	151.7
FC6	371.8	256.8	450.0	359.6
TC1	142.0	137.8	153.3	144.4
TC2	274.4	284.0	276.4	278.3
TC3	518.5	503.9	495.0	505.8
TFC1	58.5	106.4	127.5	97.5
TFC2	183.6	91.4	227.3	167.4
TFC3	501.9	301.1	-	401.5
TFC4	134.5	131.9	143.5	136.7
TFC5	223.9	239.2	255.6	239.6
TFC6	497.4	-	544.9	521.2

Note: "–" indicates missing data due to testing errors or compromised specimens.

TABLE VIII
Average compressive strength by specimen diameter and steel fibre content

Specimen diameter (mm)	Without PVC tube			With PVC tube		
	0% SF	0.75% SF	1.5% SF	0% SF	0.75% SF	1.5%SF
75	101.0	84.1	83.3	144.4	97.5	136.7
100	214.5	155.4	151.7	278.3	167.4	239.6
150	495.2	455.8	359.6	505.8	401.5	521.2

Note: SF – Steel fibre

TABLE IX
Rate of strength increment as the specimen diameter increased from 75 mm to 150 mm

Category	Details	*d* = 75 mm	*d* = 150 mm	Increase ratio
Geometry of Specimens	Cross-sectional area	4418 mm²	17671 mm²	4.0 times
Compressive Strength (without PVC tube)	0% fibre	101.0 N/mm²	495.2 N/mm²	4.9 times
	0.75% fibre	84.1 N/mm²	455.8 N/mm²	5.4 times
	1.5% fibre	83.3 N/mm²	359.6 N/mm²	4.3 times
Compressive Strength (with PVC tube)	0% fibre	144.4 N/mm²	505.8 N/mm²	3.5 times
	0.75% fibre	97.5 N/mm²	401.5 N/mm²	4.1 times
	1.5% fibre	136.7 N/mm²	521.2 N/mm²	3.8 times

Note: Increase ratio indicates how many times greater the 150 mm specimen strength or area is compared to the 75 mm specimen.

However, the strength increase was not exactly fourfold in all cases, indicating that factors beyond cross-sectional area were at play. One such factor was the slenderness ratio (*h/d*), where *h* is specimen height and *d* is diameter. Specimens with diameters of 75 mm and 150 mm had *h/d* ratios of 4.1 and 2, respectively. A higher slenderness ratio increased the risk of buckling, slightly reducing axial strength. For unconfined specimens, the increase in diameter resulted in both a fourfold increase in cross-sectional area and a lower *h/d* ratio. Together, these factors contributed to strength gains of at least 4.3 times across all fibre contents (0%, 0.75%, and 1.5%).

In confined specimens, another influencing factor was the effectiveness of tube confinement, represented by the 2*t/d* ratio, where *t* is tube thickness and *d* is diameter. According to Woldemariam et al. (2019), confinement effectiveness increases with a higher 2*t/d* ratio. As diameter increased, the 2*t/d* ratio decreased, allowing greater lateral expansion of the concrete under compression and reducing resistance to that expansion. This weakened the confinement effect and limited the strength gain (Yii and Ling, 2024).

Thus, increasing the diameter reduced both the 2*t/d* and *h/d* ratios. While the lower 2*t/d* ratio weakened confinement and was unfavourable for strength, the lower *h/d* ratio reduced buckling risk and was favourable. These opposite effects produced a mixed outcome: unlike the unconfined specimens, the strength enhancement of the confined specimens did not consistently exceed four times, despite the fourfold increase in cross-sectional area.

The interplay among three factors, namely (a) increasing cross-sectional area, (b) decreasing *h/d* ratio, and (c) decreasing 2*t/d* ratio, helps explain the different strength gains between confined and unconfined specimens as diameter increased from 75 mm to 150 mm.

Although confined specimens exhibited higher absolute strength, their proportional strength gains were smaller than those of unconfined specimens. Unconfined specimens fully benefited from the increased cross-sectional area and reduced slenderness ratio (*h/d*), without the limiting effect of reduced confinement effectiveness. In contrast, confined specimens showed diminished confinement effectiveness at larger diameters due to lower 2*t/d* ratios, which in turn limited their strength gains.

Effect of Steel Fibre Content

Steel fibres generally reduced the compressive strength of concrete. Most specimens with 0.75% and 1.5% steel fibre showed lower compressive strength than those without fibre, both with and without PVC tubes. An exception was TFC6 (150 mm diameter, 1.5% fibre with PVC tube), which showed a slightly higher strength, about 3% more than its unconfined counterpart.

Dividing the compressive strength of specimens with steel fibres by that of specimens without steel fibres (of the same diameter) gives a ratio ranging from 0.71 to 0.92 for specimens without PVC tubes, and from 0.60 to 1.03 for those with PVC tubes (Table X). This fluctuation reflects the inconsistent effect of steel fibre inclusion on compressive strength, likely due to random and uneven fibre distribution or reduced workability, which can weaken the bond within the concrete matrix.

TABLE X
Strength ratio of specimens with respect to specimens with 0% fibre

Specimen diameter (mm)	Without PVC tube		With PVC tube	
	0.75% SF	1.50% SF	0.75% SF	1.50% SF
75	0.83	0.82	0.68	0.95
100	0.72	0.71	0.60	0.86
150	0.92	0.73	0.79	1.03

*Strength ratio = compressive strength of specimens with fibres / compressive strength of specimens without fibres.

The wider variation observed in specimens with PVC tubes suggests greater inconsistency under confinement compared to unconfined specimens. This may be attributed to the combined effects of reduced workability, uneven fibre distribution, and the interaction between the confining PVC tube and the irregular fibre network. Confinement may intensify local stress concentrations caused by fibre misalignment or clustering, leading to more variable performance.

These experimental observations are consistent with findings in the literature. Tao et al. (2007) reported that adding steel fibres had only a moderate effect on the ultimate strength of concrete-filled steel tube (CFST) columns, but significantly improved ductility due to enhanced compressive behaviour and post-cracking tensile strength. Similarly, Liao et al. (2015) found that while steel fibres can increase strain capacity and post-peak response, particularly in high-strength concrete, they do not significantly enhance compressive strength or the tangent modulus. These studies support the notion that steel fibres consistently contribute more to ductility than to compressive strength. This aligns with the intended role of steel fibre reinforced concrete (SFRC), which is primarily designed to improve

ductility by delaying the onset of tensile cracks, limiting crack propagation, and enhancing tensile strength and toughness (Ulas et al., 2017).

Steel fibres have good tensile properties but are less effective in enhancing compressive strength. The compressive strength is likely influenced more by the restriction of lateral expansion than by direct resistance to axial load, although the fibres may still contribute to some extent. This explains the typically modest and inconsistent improvements in compressive strength with steel fibre inclusion. In this study, any potential strength gain was likely offset by poor workability and uneven fibre distribution in the mix.

Effect of PVC Tube

Specimens with PVC tubes generally showed higher compressive strength than those without, especially at 1.5% steel fibre (Table VIII). At this fibre content, strength increased by 64%, 58%, and 45% for specimens with diameters of 75 mm, 100 mm, and 150 mm, respectively.

Under compression, concrete undergoes elastic shortening, which causes lateral expansion. The PVC tube restricted this expansion through its tensile resistance along the perimeter, creating a triaxial confinement condition. This confinement slowed microcrack propagation and improved compressive strength.

At 0.75% fibre content, strength improvements by PVC tubes were lower: 16%, 8%, and –12% for 75 mm, 100 mm, and 150 mm specimens, respectively. In contrast, 1.5% fibre content resulted in significant improvements of 64%, 58%, and 45%. This indicates that 0.75% was insufficient to enhance confinement, while 1.5% allowed better synergy between internal reinforcement from steel fibres and external confinement from the PVC tube.

Failure mode

Three main failure modes were observed among the confined specimens TC and TFC: shear, bulging, and tube bursting (Table XI and Figure 6). Bulging was the most frequent failure mode, followed by shear. Tube bursting was the least common, occurring only in one of the three TFC1 specimens.

Bulging failure occurred when the concrete core experienced excessive lateral dilation, likely due to internal crushing and damage, combined with significant axial shortening. This caused the PVC tube to deform outward and also shorten. The observed plastic deformation of the tube indicated that its elastic limit had been exceeded, suggesting that the tube actively resisted the concrete's lateral expansion. Such a failure mode reflects ductile behaviour, where the confinement delayed sudden collapse after peak strength by allowing gradual deformation. It is generally considered a desirable failure mode for confined concrete.

TABLE XI
Failure Mode of Specimens (Confined)

Specimen	Sample 1	Sample 2	Sample 3	Primary failure mode
TC1	Bulging (top)	Bulging (top)	Bulging (top)	Bulging
TC2	Bulging (top)	Bulging (top)	Bulging (top)	Bulging
TC3	Shear	Shear	Bulging (top)	Shear
TFC1	Tube bursting	Bulging (bottom)	Bulging (top)	Bulging
TFC2	Bulging (bottom)	Bulging (top)	Bulging (Middle)	Bulging
TFC3	Shear	Shear	Bulging (top)	Shear
TFC4	Bulging (top)	Bulging (top)	Shear	Bulging
TFC5	Shear	Shear	Shear	Shear
TFC6	Shear	Shear	Shear	Shear

Note: The primary failure mode was identified based on the most commonly observed failure among the three identical specimens.

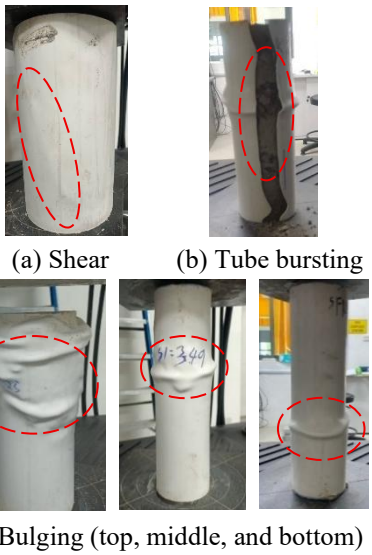

(a) Shear (b) Tube bursting

(c) Bulging (top, middle, and bottom)

Figure 6. *Typical failure modes of confined specimens TC and TFC*

Shear failure was characterized by diagonal cracking and abrupt material displacement along inclined planes within the concrete. Under axial loading, the concrete initially underwent elastic shortening, during which microcracks developed

once the strain limit was exceeded. As the load increased, these microcracks propagated and merged into larger cracks, gradually forming a shear plane due to the combined effects of axial shortening and lateral expansion. When the internal shear stresses surpassed the concrete's shear resistance, failure occurred along the inclined plane. This mode reflects a brittle response, typically associated with inadequate confinement or insufficient fibre bridging, and often results in a sudden loss of load-carrying capacity.

Tube bursting involved the rupture or tearing of the confining PVC tube due to excessive lateral expansion of the concrete core. This expansion was likely caused by severe internal damage, including excessive elastic shortening, crushing, or splitting of the concrete under axial load. The resulting internal pressure generated high tensile hoop stresses that exceeded the tensile strength of the PVC tube. Although such failure could be attributed to material defects in the tube, this possibility was ruled out based on the consistent tensile strength results of the PVC tubes shown in Table VI. Instead, this failure mode highlights the confinement effect provided by the PVC tube, confirming its active role in resisting lateral expansion. However, it ultimately failed due to insufficient tensile resistance against the internal pressure exerted by the expanding concrete.

The primary failure modes presented in Table XI were mapped based on specimen diameter and steel fibre content in Table XII to identify potential trends. Shear failure appeared more prevalent in specimens with larger diameters (150 mm) and higher fibre content (1.5%), while the remaining specimens predominantly exhibited bulging failure. Similar prevalent failure modes were reported by Woldemariam et al. (2019), namely drum-type (bulging) failure and shear-type failure.

TABLE XII
Typical failure mode by specimen diameter and steel fibre content

Specimen diameter (mm)	0% Steel Fibre	0.75% Steel Fibre	1.5% Steel Fibre
75	Bulging	Bulging	Bulging
100	Bulging	Bulging	Shear
150	Shear	Shear	Shear

Specimens with a 150 mm diameter (TC3, TFC3, and TFC6) had lower 2*t/d* ratios, resulting in weaker confinement, which resulted in shear failure. This aligns with Gupta (2013), who recommends using a lower diameter-to-thickness (*d/t*) ratio, or a higher 2*t/d* ratio, to reduce the risk of shear failure. Although TFC5 had a smaller diameter, its higher fibre content (1.5%) may have restricted elastic shortening and lateral expansion. Steel fibres enhance internal integrity by bridging microcracks and reducing deformation under axial compression. This is evident in Figure 7, where fibres are seen holding the spalled concrete together after failure. Liao et al. (2015) similarly reported that steel fibre reinforced concrete exhibited more cracks near the failure zone and reduced spalling. In TFC5, the reduced lateral expansion likely led to lower pressure on the PVC tube, limiting its confinement effect and contributing to shear-related failure.

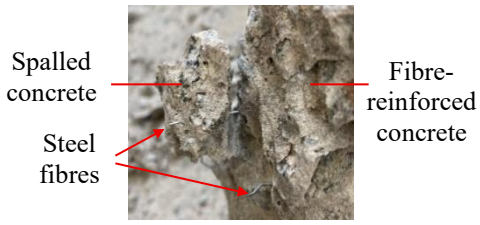

Figure 7. *Steel fibres strengthening the tensile resistance of concrete*

In contrast, bulging failure was more common among specimens with smaller diameters (≤100 mm) and lower fibre content (≤0.75%). The smaller diameter produced a higher 2*t/d* ratio, which provided more effective confinement. Additionally, the lower fibre content allowed greater lateral expansion of the concrete, thereby activating a stronger confinement response from the PVC tube.

IV. LIMITATIONS AND RECOMMENDATIONS

There is a threshold fibre content beyond which the flowability and workability of SFRC are significantly reduced. When the fibre volume exceeds this critical level, uniform distribution becomes difficult, increasing the risk of fibre interlock and clumping (Akeed et al., 2022). In this study, the optimum steel fibre content for enhancing compressive strength could not be identified. Given the generally poor workability observed, and the fact that most steel fibre specimens (except TFC6) exhibited lower compressive strength than those without fibres, it is plausible that the adverse effects on workability outweighed the relatively limited structural benefits provided by the fibres. This observation warrants further investigation to verify the interaction between fibre content, workability, and compressive strength in future studies.

No tests were conducted to directly verify fibre clumping or to quantify the severity of uneven fibre distribution in the specimens. The explanation for the reduced compressive strength observed with steel fibre inclusion was based on the assumption that poor workability increased the likelihood of such defects, as suggested by previous studies, rather than confirmed through direct evidence in this study. Similarly, the bond between steel fibres and the cement matrix was inferred based on established understanding of the strong interfacial bond typically achieved with hooked-end steel fibres, rather than measured explicitly. For a more accurate and comprehensive understanding, future studies should incorporate methods to directly assess fibre distribution, clumping, and interfacial bonding behaviour.

The combined use of SFRC and CFPT presents challenges due to limitations that hinder effective confinement. According to Ling et al. (2023a), effective confinement depends on two key conditions: (a) the tube must be rigid and strong enough to resist concrete expansion, and (b) the concrete must expand sufficiently to activate the tube. While each condition may provide some confinement, both are needed for optimal results. Ling et al. (2023b) further noted that in CFT systems, confinement may not occur if the tube expands faster than the concrete. This depends on two additional factors: (a) the absence of a gap between the concrete and the tube, and (b) the tube's yield strain not being exceeded (Ling et al., 2023b). In this study, the PVC tube had low stiffness and tensile strength, limiting its ability to resist expansion. The steel fibres likely reduced lateral expansion, making it harder for the concrete to activate the tube. These factors limited or even nullified the confinement effect. Future studies could explore ways to improve compatibility, such as using hybrid fibres to balance strength and flexibility, adding expansive agents to promote concrete expansion, or installing hoop links to restrain the tube and enhance confinement.

V. CONCLUSION

This study investigated the compressive strength behaviour of concrete specimens with varying diameters (75 mm, 100 mm, and 150 mm), steel fibre contents (0%, 0.75%, and 1.5%), and confinement conditions (with or without PVC tubes). A total of 54 specimens were prepared across four categories: C – plain concrete, FC – steel fibre reinforced concrete, TC – plain concrete with tube, and TFC – fibre reinforced concrete with tube.

Based on the experimental results and analysis, the following conclusions are drawn:

1. Compressive strength increased with specimen diameter, regardless of steel fibre content or the presence of confinement. When the diameter doubled from 75 mm to 150 mm, the cross-sectional area increased fourfold. Combined with the effects of decreasing slenderness (h/d) and confinement effectiveness ($2t/d$), the strength gain ranged from 4.3 to 5.4 times without PVC tubes and from 3.5 to 4.1 times with tubes.
2. Steel fibre inclusion generally reduced compressive strength, with inconsistent results across batches. This reduction is likely due to low workability, which may have caused uneven fibre distribution and poor compaction, weakening the concrete matrix.
3. PVC tubes enhanced compressive strength through confinement. At 1.5% steel fibre content, strength increased by 64%, 58%, and 45% for specimens with diameters of 75 mm, 100 mm, and 150 mm, respectively, compared to their unconfined counterparts. The confinement effect was more pronounced in smaller-diameter specimens due to higher $2t/d$ ratios.
4. Three failure modes were observed: bulging, shear, and tube bursting. Shear failure was more prevalent in specimens with larger diameters (150 mm) and higher fibre content (1.5%), while bulging was more common in smaller specimens (≤100 mm) with lower fibre content (≤0.75%). Bulging failure indicates a more effective engagement of the confinement mechanism compared to shear failure.

These findings highlight the importance of considering both geometric parameters and material behaviour in optimizing the compressive performance of confined and fibre-reinforced concrete.

ACKNOWLEDGEMENT

This research work was funded by the Research Grants of University of Technology Sarawak UTS/Research/<2/2025/07>.

REFERENCE

Abdulla, N. A. 2017. Concrete filled PVC tube: A review. Construction and Building Materials, 156, pp. 321–329. https://doi.org/10.1016/j.conbuildmat.2017.08.156

Akeed, M. H., Qaidi, S., Ahmed, H. U., Emad, W., Faraj, R. H., Mohammed, A. S., Tayeh,

B. A. and Azevedo, A. R. G. 2022. Ultra-high-performance fiber-reinforced concrete. Part III: Fresh and hardened properties. Case Studies in Construction Materials, 17, p. e01265. https://doi.org/10.1016/j.cscm.2022.e01265

Azeez, A. A., Jamaluddin, N., Rahman, N. A., Hassen, D. R. and Attiyah, A. N. 2018. Experimental and analytical study of PVC confined concrete cylinders. Journal of Engineering and Applied Sciences, 13, pp. 2145–2151.

Bandyopadhyay, A., Chanu, Y. M. and Samanta, A. K. 2019. Experimental investigation on mechanical properties of PCC and FRC confined with UPVC pipe. Indian Journal of Engineering & Materials Sciences, 26, pp. 342–348.

El-Dieb, A. S. and Reda Taha, M. M. 2012. Flow characteristics and acceptance criteria of fiber-reinforced self-compacted concrete (FR-SCC). Construction and Building Materials, 27(1), 585–596. https://doi.org/10.1016/j.conbuildmat.2011.07.004

Fakharifar, M. and Chen, G. 2016. Compressive behavior of FRP-confined concrete-filled PVC tubular columns. Composite Structures, 141, pp. 91–109. https://doi.org/10.1016/j.compstruct.2016.01.004

Fakharifar, M. and Chen, G. 2017. FRP-confined concrete filled PVC tubes: A new design concept for ductile column construction in seismic regions. Construction and Building Materials, 130, 1–10. https://doi.org/10.1016/j.conbuildmat.2016.11.056

Gupta, P. K. 2013. Confinement of concrete columns with unplasticized poly-vinyl chloride tubes. International Journal of Advanced Structural Engineering, 5, p. 19. https://doi.org/10.1186/2008-6695-5-19

He, L., Zhao, Y. and Lin, S. 2018. Experimental study on axially compressed circular CFST columns with improved confinement effect. Journal of Constructional Steel Research, 140, 74–81. https://doi.org/10.1016/j.jcsr.2017.10.025

Hoang, A. L., Fehling, E., Lai, B., Thai, D.-K. and Chau, N. V. 2019. Experimental study on structural performance of UHPC and UHPFRC columns confined with steel tube. Engineering Structures, 187, pp. 457–477. https://doi.org/10.1016/j.engstruct.2019.02.063

Khaloo, A., Molaei Raisi, E., Hosseini, P. and Tahsiri, H. 2014. Mechanical performance of self-compacting concrete reinforced with steel fibers. Construction and Building Materials, 51, pp. 179–186. https://doi.org/10.1016/j.conbuildmat.2013.10.054

Liao, W.-C., Perceka, W. and Liu, E.-J. 2015. Compressive stress-strain relationship of high strength steel fiber reinforced concrete. Journal of Advanced Concrete Technology, 13(8), pp. 379–392. https://doi.org/10.3151/jact.13.379

Liew, J. Y. R. and Xiong, D. X. 2012. Ultra-high strength concrete filled composite columns for multi-storey building construction. Advances in Structural Engineering, 15(9), pp. 1487–1503. https://doi.org/10.1260/1369-4332.15.9.1487

Ling, J. H., Lim, Y. T., Leong, W. K. and Sia, H. T. 2023a. Concrete-filled tubular column made of various types of material. Journal of Civil Engineering, 38(1), pp. 3–15. http://dx.doi.org/10.12962/j20861206.v38i1.15455

Ling, J. H., Lim, Y. T., Leong, W. K. and Sia, H. T. 2023b. Learning about concrete-filled tube using ChatGPT. Journal of Civil Engineering, 38(1), pp. 54–64. http://dx.doi.org/10.12962/j20861206.v38i1.16470

Ling, J. H. and Omoregie, A. I. 2025. A bibliometric overview of current states and research trends in concrete-filled tube columns. Journal of Civil Engineering, 40(2), pp. 191–210. http://dx.doi.org/10.12962/j20861206.v40i2.22784

Lu, Y., Li, N., Li, S. and Liang, H. 2015. Behavior of steel fiber reinforced concrete-filled steel tube columns under axial compression. Construction and Building Materials, 95, pp. 74–85. https://doi.org/10.1016/j.conbuildmat.2015.07.114

Mohammad Askari, S., Khaloo, A., Borhani, M. H. and Tale Masoule, M. S. 2020. Performance of polypropylene fiber reinforced concrete-filled UPVC tube columns under axial compression. Construction and Building Materials, 231, p. 117049. https://doi.org/10.1016/j.conbuildmat.2019.117049

Nedeljković, M., Visser, J., Šavija, B., Valcke, S. and Schlangen, E. 2021. Use of fine recycled concrete aggregates in concrete: A

critical review. Journal of Building Engineering, 38, pp. 102196. https://doi.org/10.1016/j.jobe.2021.102196

Nunna, S., Ravindran, A. R., Mroszczok, J., Creighton, C. and Varley, R. J. 2023. A review of the structural factors which control compression in carbon fibres and their composites. Composite Structures, 303, p. 116293. https://doi.org/10.1016/j.compstruct.2022.116293

Pham, T. M. 2025. Fibre-reinforced concrete: State-of-the-art review on bridging mechanism, mechanical properties, durability, and eco-economic analysis. Case Studies in Construction Materials, 22, p. e04574. https://doi.org/10.1016/j.cscm.2025.e04574

Tao, Z., Han, L.-H. and Wang, D.-Y. 2007. Experimental behaviour of concrete-filled stiffened thin-walled steel tubular columns. Thin-Walled Structures, 45(5), pp. 517–527. https://doi.org/10.1016/j.tws.2007.04.003

Ulas, M. A., Alyamac, K. E. and Ulucan, Z. C. 2017. Effects of aggregate grading on the properties of steel fibre-reinforced concrete. IOP Conference Series: Materials Science and Engineering, 246, p. 012015. https://doi.org/10.1088/1757-899X/246/1/012015

Wang, J.-Y. and Yang, Q.-B. 2012. Investigation on compressive behaviors of thermoplastic pipe confined concrete. Construction and Building Materials, 35, pp. 578–585. https://doi.org/10.1016/j.conbuildmat.2012.04.017

Wang, W., Shen, A., Lyu, Z., He, Z. and Nguyen, K. T. Q. 2021. Fresh and rheological characteristics of fiber reinforced concrete: A review. Construction and Building Materials, 296, p. 123734. https://doi.org/10.1016/j.conbuildmat.2021.123734

Wang, X., Fan, F. and Lai, J. 2022. Strength behavior of circular concrete-filled steel tube stub columns under axial compression: A review. Construction and Building Materials, 322, p. 126144. https://doi.org/10.1016/j.conbuildmat.2021.126144

Woldemariam, A. M., Oyawa, W. O. and Nyomboi, T. 2019. Structural performance of uPVC confined concrete equivalent cylinders under axial compression loads. Buildings, 9(4), 82. https://doi.org/10.3390/buildings9040082

Wu, Z., Shi, C., He, W. and Wu, L. 2016. Effects of steel fiber content and shape on mechanical properties of ultra-high performance concrete. Construction and Building Materials, 103, pp. 8–14. https://doi.org/10.1016/j.conbuildmat.2015.11.028

Yii, P. Z. F. and Ling, J. H. 2024. Behaviour of concrete-filled plastic tube (CFPT) embedded with reinforcement bar under axial compressive load. Borneo Journal of Sciences and Technology, 6(1), pp. 28–38. https://doi.org/10.35370/bjost.2024.6.1-04

Zheng, S., Liu, T., Jiang, G., Fang, C., Qu, B., Gao, P., Li, L. and Feng, Y. 2021. Effects of water-to-cement ratio on pore structure evolution and strength development of cement slurry based on HYMOSTRUC3D and micro-CT. Applied Sciences, 11(7), p. 3063. https://doi.org/10.3390/app11073063